Applied Catalysis A: General 517 (2016) 161–167

Contents lists available at ScienceDirect

Applied Catalysis A: General

journal homepage: www.elsevier.com/locate/apcata

Hydrogen peroxide electrogeneration in gas diffusion electrode nanostructured with Ta_2O_5

Jussara F. Carneiro[a], Robson S. Rocha[a], Peter Hammer[b], R. Bertazzoli[c], M.R.V. Lanza[a,*]

[a] Instituto de Química de São Carlos, Universidade de São Paulo, Avenida Trabalhador São Carlense 400, 13566-590 São Carlos, SP, Brazil
[b] Instituto de Química, Universidade Estadual Paulista, Rua Professor Francisco Degni 55, 14800-060 Araraquara, SP, Brazil
[c] Faculdade de Engenharia Mecânica, Universidade Estadual de Campinas, Rua Mendeleyev 200, 13083-860 Campinas, SP, Brazil

ARTICLE INFO

Article history:
Received 30 December 2015
Received in revised form 23 February 2016
Accepted 9 March 2016
Available online 11 March 2016

Keywords:
Tantalum oxide
Oxygen reduction reaction
Hydrogen peroxide electrogeneration
Gas diffusion electrode

ABSTRACT

Highly efficient H_2O_2 electrogeneration is required in the Advanced Oxidation Process for organic wastewater treatment. However, the development of more efficient catalytic particles used in gas diffusion electrodes (GDEs) to enable the oxygen reduction reaction through two-electron transfer is still of great importance. The performance of the Ta_2O_5 nanoparticles on carbon black in catalyzing the ORR was evaluated using rotating ring-disk electrode. The current efficiency for H_2O_2 electrogeneration on Ta_2O_5/C catalyst is 83.2% whereas carbon black exhibits 65.3%. GDEs were constructed using carbon black either unmodified or modified with Ta_2O_5 nanoparticles. The modified GDE produces 27.9 mg L^{-1} of H_2O_2, while the unmodified GDE generates 19.1 mg L^{-1} of H_2O_2. Furthermore, the energy consumption for the H_2O_2 electrogeneration is lower in modified than in unmodified GDE (15.0 kW h vs. 18.8 kW h). The high performance of the GDE (Ta_2O_5/C) renders it a viable alternative cathode in the electrochemical treatment of wastewaters.

1. Introduction

Advanced oxidation processes (AOPs) constitute a promising technology for the treatment of wastewaters. These processes involve the generation of highly reactive species, particularly the hydroxyl radical (•OH). The •OH exhibits strong oxidizing power in aqueous phase due to its high standard reduction potential (+2.73 V *vs* SHE) [1]. Therefore, this radical is able to oxidize a wide variety of organic compounds to yield CO_2, H_2O and inorganic ions from heteroatoms [3,4]. Hydrogen peroxide, a chemical source of •OH, can be produced electrochemically using gas diffusion electrodes (GDEs) [4–6] in which this oxidant is generated at the electrode-gas-solution interface via the oxygen reduction reaction (ORR).

Under acid conditions, the oxygen can be reduced following two different paths: the first one involving four-electron transfer, H_2O production, and the second one through a two-electron transfer, H_2O_2 electrogeneration [7]. According to Griffith, Pauling and Bridge models [8], the possible reaction routes and the number of electrons transferred during the oxygen reduction process are related to the different types of O_2 adsorption on the catalytic surface. It is well known that amorphous carbon displays catalytic activity to H_2O_2 production [5]. However, the treatment of the carbon or addition of organic and inorganic materials on this substrate can enable the ORR following a two-electron pathway with high selectivity and at low overpotential [9–11].

Tantalum oxide-based catalysts exhibit high oxygen reduction onset potential (~0.95 V vs. SHE) and excellent stability under corrosive environments [12,13]. Furthermore, this oxide has acid sites [14], which promotes more hydrophilicity on the composite surface inducing more active sites for the catalytic redox reaction [15]. Therefore, in this study we investigate on the properties of Ta_2O_5/C for the electrocatalysis of oxygen reduction by rotating ring-disk electrode. The yield of H_2O_2 production and the energy consumed during the process were determined using a GDE either unmodified or modified with Ta_2O_5.

2. Experimental

2.1. Preparation of electrocatalysts

Ta_2O_5 nanoparticles supported on carbon black (Printex 6L carbon, Evonik) were prepared by thermal decomposition of a polymeric precursor solution (DPP) [16] using tantalum(V) ethoxide [$(CH_3CH_2O)_5Ta$, Sigma–Aldrich] as the salt precursor. In a typical experiment, $(CH_3CH_2O)_5Ta$, citric acid and ethylene glycol were mixed in molar ratio 1:10:40, respectively, and stirred with a mag-

* Corresponding author.
E-mail address: marcoslanza@iqsc.usp.br (M.R.V. Lanza).

http://dx.doi.org/10.1016/j.apcata.2016.03.013
0926-860X/

netic stirrer for 40 min at 60 °C. Carbon black was then added slowly to the mixture under stirring. The dispersion was heated in air at a rate of 2.5 °C min^{-1} and finally held at 500 °C for 30 min. The catalyst was prepared with 5.0% (w/w) Ta/C.

The upper temperature limit for the synthesis of nanoparticles on the carbon surface was determined by thermogravimetric analysis (TGA) of sample of carbon black using a DuPont Instruments model TGA 2950 analyzer.

In addition, carbon black was treated following the same procedure described above but without adding metallic precursor in the first step. This procedure was performed in order to verify the influence of the polymeric precursor method in the carbon catalytic activity for the ORR.

2.2. Chemical physical characterization of electrocatalysts

The morphological and chemical characterization were performed by transmission electron microscopy (TEM) and X-ray photoelectron spectroscopy (XPS). The TEM images were recorded using a 200 kV high resolution FEI Tecnai G2 F20 instrument. X-ray photoelectron spectra were measured at a pressure of less than 10^{-7} Pa using a UNI-SPECS UHV system equipped with an MgKα X-ray source (hν = 1253.6 eV) with the analyzer pass energy set at 10 eV. The inelastic background of the C (1s) and O (1s) electrons of the core-level spectra was subtracted using Shirley's method. The spectra were fitted without placing constraints using multiple Voigt profiles.

2.3. Electrochemical characterization of electrocatalysts

Electrochemical characterization were performed using a Metrohm-Autolab PGSTAT 128N potentiostat/galvanostat and a Pine Instruments rotating ring-disk electrode (RRDE) system. The working electrode was prepared by dispersing 1 mg of catalyst in 1 mL of water by sonication for 30 min and loading a 20 μL sample of the resulting suspension onto a 5.6 mm diameter glassy carbon electrode. The layer of catalyst was dried slowly in air, following which a 20 μL aliquot of an aqueous solution of Nafion® (0.05%) was transferred carefully to the microlayer surface. Experiments were carried out in a conventional electrochemical cell using Pt foil as counter electrode, an Ag/AgCl electrode as reference electrode and an electrolyte solution comprising 0.1 mol L^{-1} K_2SO_4 at pH = 2, adjusted by H_2SO_4.

Cyclic voltammetry (CV) curves were recorded in N_2-saturated electrolyte solution at a sweep rate of 10 mV s^{-1}. The linear sweep voltammetry (LSV) curves were conducted in N_2 and O_2-saturated solution. The disk electrode was scanned at a rate of 5 mV s^{-1} while the ring potential was kept constant at +1.0 V. All the LSVs curves presented in this work were corrected by subtracting of the background current recorded in N_2-satured solution.

2.4. Generation of H_2O_2 in a gas diffusion electrode

Based on the results obtained from the RRDE experiments, GDE with 3.4 cm^2 exposed area were constructed with carbon black either unmodified or modified with Ta2O5 nanoparticles (5.0% (w/w) Ta/C) and 20% (w/w) of a 60% aqueous dispersion of DuPont Teflon® PTFE TE 3859 as described previously [6,7].

Electrochemical experiments were performed in a three-electrode single compartment cell with the working electrode (GDE) located at the bottom of the cell and supplied with O_2 at a pressure of 0.2 bar. In order to quantify the H_2O_2 produced during electrolysis, 0.5 mL samples of electrolyte were collected at appropriate time intervals, mixed with 4 mL aliquots of a solution of $(NH_4)_6Mo_7O_{24}$ (2.4×10^{-3} mol L^{-1}) in 0.5 mol L^{-1} H_2SO_4 and absorption measured at 350 nm. The amounts of H_2O_2 present in the samples were evaluated by reference to a standard calibration curve [9,17].

3. Results and discussion

3.1. Characterization of electrocatalysts

The TGA analysis of carbon black (Fig. S1) represents the weight loss of a sample as a function of temperature. The small (2%) reduction in weight observed on heating from 25 °C to ~500 °C can be associated with the loss of water adsorbed on the carbon. However, heating to temperatures above 600 °C give rise to a pronounced loss in weight of carbon black and it is fully degraded to CO_2 at 700 °C. These results provided an upper temperature limit (taken as 500 °C) for the thermal treatment employed in the synthesis of nanoparticles on the surface of carbon black.

TEM images of Ta_2O_5 on carbon black are shown in Fig. 1. These images show the good distribution of Ta_2O_5 nanoparticles over the carbon (Fig. 1A and B) with a particle size around 2.07 ± 0.27 nm (Fig. 1C). The selective area diffraction pattern (SAED, Fig. 1D), with well-defined lattice planes, confirms the nanocrystalline structure of the Ta_2O_5 nanoparticles. The interplanar distance of 3.36 Å and 3.63 Å correspond to the (0 1 5) and (0 1 3) planes (JCPDS#27-1447), respectively. Furthermore, elemental mapping of Ta, C and O using energy dispersive X-ray analysis was undertaken (Fig. 1E–H and Fig. S2). The area of bright contrast correlates with the Ta signal map.

Fig. 2A and B shows the respective fitted high resolution XPS C (1s) spectra for carbon black before and after thermal treatment by polymeric precursor method. The four components present in the deconvoluted spectra are associated with the aromatic phase (C—C sp^2) centered at 284.3 eV, C—H carbon at 285.4 eV and the oxidized carbon groups in the form of carbonyl (C═O) at 287.3 eV and carboxyl (O—C═O) at 289.3 eV [18]. The main component of the spectrum obtained prior to thermal treatment relates to the aromatic phase along with a small contribution from the oxygenated groups and a π plasmon peak at the high energy tail (~291 eV). However, the strong oxidation processes associated with calcination at 500 °C give rise to a marked reduction in the aromatic phase and an increase in the proportion of oxygenated groups. In fact, the oxygen concentration in the form of carbonyl and carboxyl increase from 9.2 ± 0.4 at.% to 16.9 ± 0.8 at.%. It is important to note that, according to the results obtained by TGA, the carbon black remains thermally stable at 500 °C and does not undergo combustion to CO_2.

The main components of the deconvoluted XPS O (1s) spectrum of treated carbon black (Fig. 2C) can be attributed to C═O at 532.5 eV and O—C═O at 533.9 eV [18], confirming the presence of groups previously identified in the C (1s) spectrum. An additional small component at low binding energy (530.6 eV) is present in the deconvoluted XPS O (1s) spectrum of Ta_2O_5/C electrocatalyst (Fig. 2D), and it is related to O-Ta bonds [18] of Ta_2O_5 nanoparticles embedded in the carbon matrix.

Fig. 3 shows the Ta (4f) spectrum for the Ta_2O_5/C electrocatalyst. The spectrum is fitted with very good precision by only one spin-orbit doublet at a fixed separation of 1.8 eV. The binding energy of the Ta 4f7/2 centered at 27.1 eV corresponds to the Ta_2O_5 phase [18]. This result, combined with the SAED pattern, provides a clear evidence for the presence of Ta_2O_5 on the carbon surface.

3.2. Study of the reduction reaction of molecular oxygen

Fig. 4 shows the cyclic voltammograms obtained for uncoated disk electrode (glassy carbon), treated and non-treated carbon black and Ta_2O_5/C electrodes in N_2-saturated solution. The voltammogram of the carbon black shows no peak of redox transition

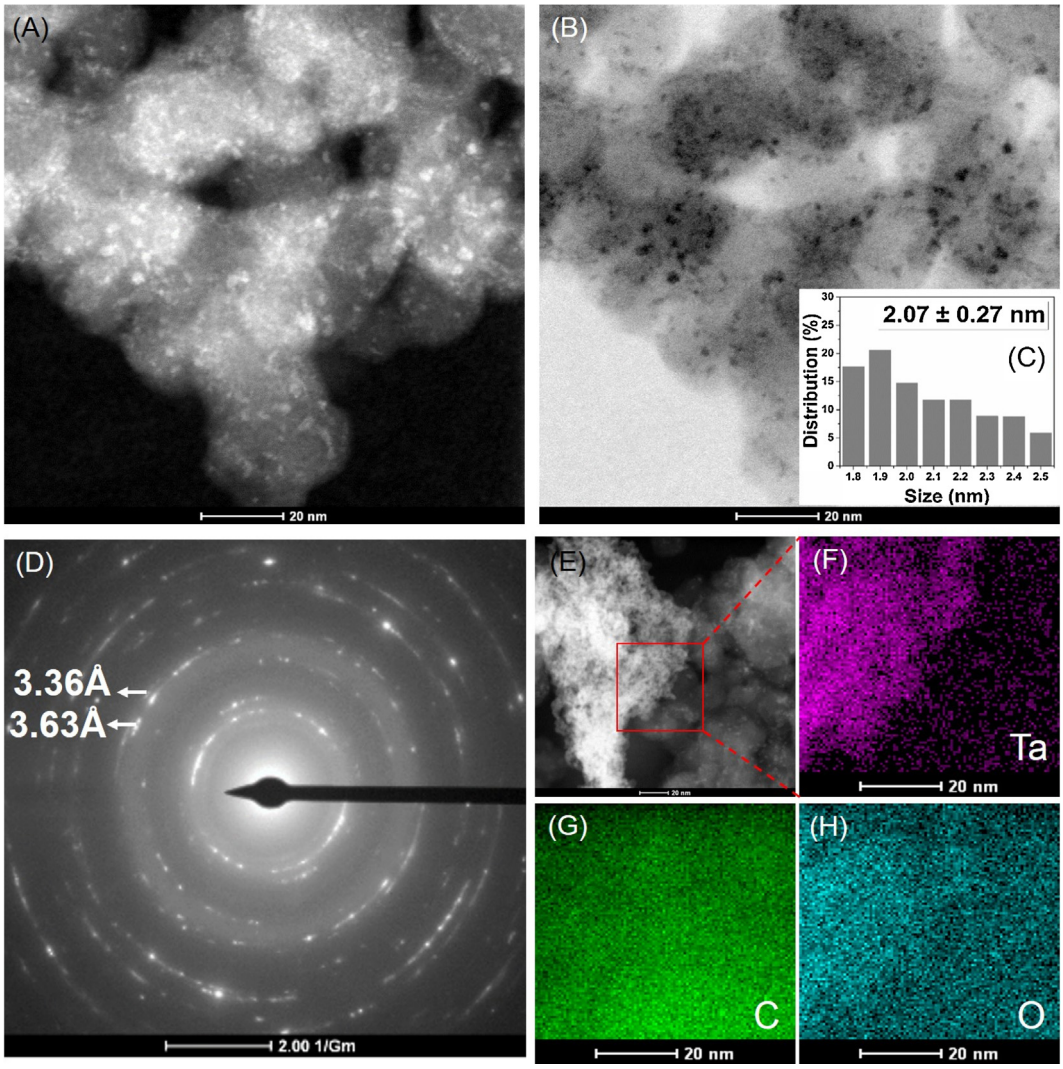

Fig. 1. TEM image of Ta_2O_5 supported on carbon black: (A) dark field and (B) bright field; (C) estimated particle size; (D) SAED pattern of the Ta_2O_5/C; (E) scanning TEM and elemental mapping images of (F) Ta, (G) C and (H) O.

(Fig. 4, plot b). However, a blurred peak at ca. +0.1 V is observed in the CV after thermal treatment of the carbon (Fig. 4, plot c and inserted). This redox transition can be attributed to the increase of oxygenated groups on the treated carbon surface in agreement with XPS analysis [6,19–21].

The voltammogram for the Ta_2O_5/C electrode (Fig. 4, plots d) shows a blurred peak from +0.4 V to 0.0 V. This redox transition can be assigned to the reduction of Ta_2O_5 to metallic Ta (Eq. (1)) in agreement with potential-pH equilibrium diagram for tantalum-water, at 25 °C, described by Pourbaix [22] and the presence of oxygenated groups on the catalytic surface [19].

$$Ta_2O_5 + 10H^+ + 10e^- \rightleftarrows 2Ta + 5H_2O \quad (1)$$

The variation in current values at potentials lower than −0.4 V is related to the start of the hydrogen evolution reaction arising from the reduction of H^+ ions present in solution.

In order to verify the ORR pathway of the carbon black, treated carbon and Ta_2O_5/C catalysts, the formation of H_2O_2 (ring current—I_{ring}) was monitored using a RRDE system. As shown in Fig. 5, the treated carbon black displays higher ring current than the non-treated carbon demonstrating that the increase in the oxygen-containing functional groups on the carbon surface (XPS data) makes the catalyst more selective for H_2O_2 electrogeneration.

Linear voltammetric profiles of the Ta_2O_5/C catalyst show oxidation currents of hydrogen peroxide (I_{ring}) higher than those of carbon black, suggesting higher H_2O_2 electrogeneration in the presence of Ta_2O_5. Furthermore, this catalyst exhibit overpotential 97 mV lower than that of carbon black for the reduction O_2 to H_2O_2, thus enabling the two-electron ORR pathway at lower overpotential. The shift in the ORR onset potential in the presence of Ta_2O_5 can be explain by the high ORR onset potential of this oxide [12,13].

The current efficiency for hydrogen peroxide formation ($I(H_2O_2)\%$) and the number of electrons transferred (n_t) during the oxygen reduction were determined quantitatively using the following equations [23]:

$$I(H_2O_2)\% = \frac{200 \cdot I_r/N}{I_d + I_r/N} \quad (2)$$

$$n_t = \frac{4 \times I_d}{I_d + I_r/N} \quad (3)$$

where I_r is the ring current, I_d is the disk current and N is the current collection efficiency of the Pt ring (N = 0.37). The values of $I(H_2O_2)\%$ and n_t obtained for the electrocatalysts employed in this study are shown in Table 1.

According to Table 1, the H_2O_2 production on carbon black is 65.3% whereas on treated carbon black is 74.5%. Moreover, the

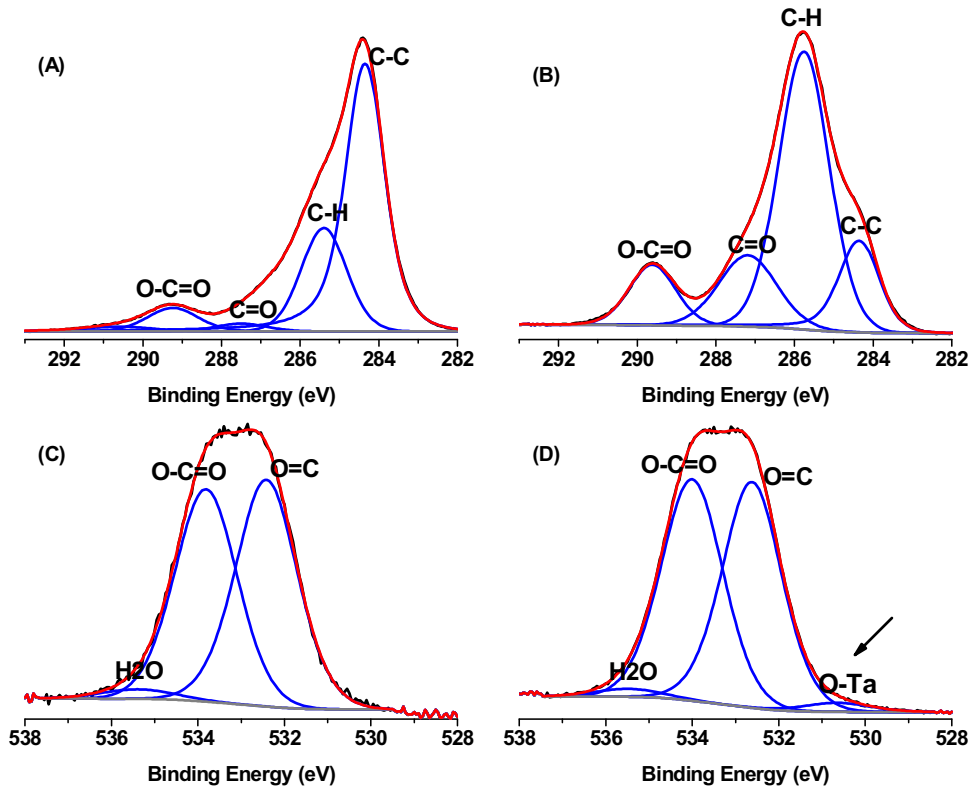

Fig. 2. Deconvoluted XPS C (1s) spectra of (A) carbon black and (B) treated carbon black. Deconvoluted XPS O (1s) spectra of (C) treated carbon black and (D) Ta_2O_5/C electrocatalyst (5.0% w/w Ta/C).

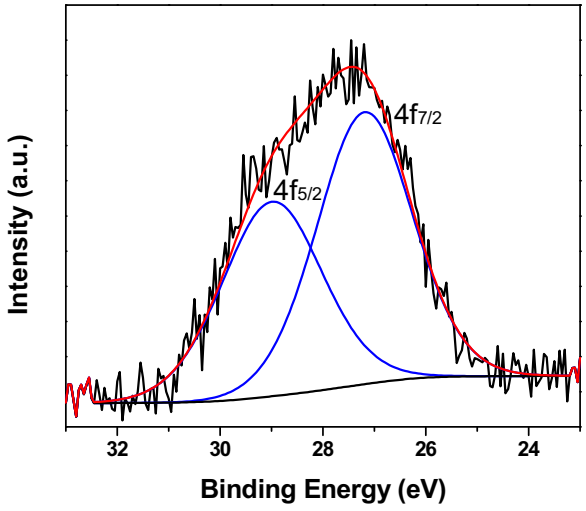

Fig. 3. Deconvoluted Ta (4f) spectrum of Ta_2O_5/C electrocatalyst (5.0% w/w Ta/C).

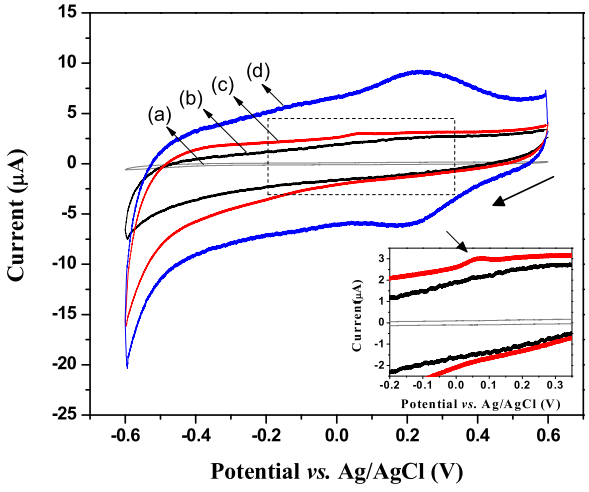

Fig. 4. Cyclic voltammetric profiles of (a) uncoated disk electrode (glassy carbon), (b) carbon black (c) treated carbon black and (d) Ta_2O_5/C electrodes recorded in N_2-saturated solution 0.1 mol L^{-1} K_2SO_4 at pH = 2, adjusted by H_2SO_4, at a scan rate of 10 mV s^{-1}.

Table 1
Current efficiency for hydrogen peroxide formation and number of electrons transferred during the ORR. The values presented were calculated over the potential range from −0.3 V to −0.5 V (region of mixed control of the LSVs).

	Carbon black	Treated carbon black	Ta_2O_5/C(5.0% (w/w) Ta/C)
I(H_2O_2)%	65.3	74.5	83.2
nt	2.7	2.5	2.3

presence of Ta_2O_5 increase the selectivity for H_2O_2 electrogeneration to 83.2%. Therefore, the high selectivity to H_2O_2 production on Ta_2O_5/C catalyst is atttributed to the synergistic effect between the Ta_2O_5 nanoparticles and the oxygen functional groups on the surface of the material. In this context, the presence of Ta_2O_5 promotes RRO via electrochemical/chemical mechanism. In the electrochemical stage, Ta_2O_5 is reduced in the cathode sweep [22]. Then, the oxygen molecule absorbs on the catalyst surface as described in the Pauling model [8] in which oxygen is reduced causing the oxidation of tantalum (chemical step). Additionally, the presence of oxygen functional groups on the material surface act as electroactive sites promoting the transfer of electrons for the ORR [19].

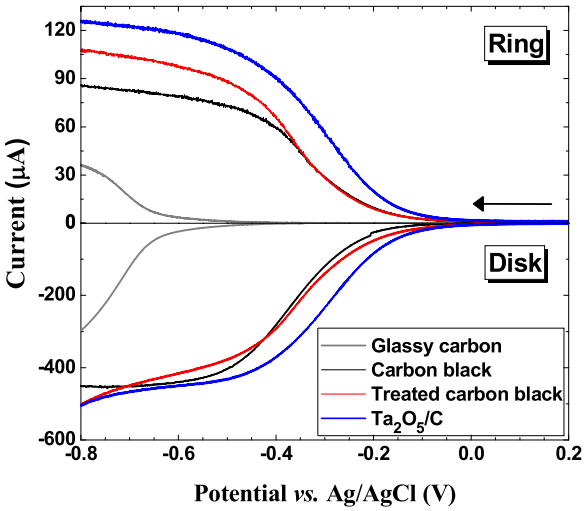

Fig. 5. Steady state polarization curves for the ORR determined using RRDE system of uncoated disk electrode, carbon black, treated carbon black and Ta_2O_5/C (5.0% (w/w) Ta/C) catalysts. The electrolyte was 0.1 mol L^{-1} K_2SO_4 at pH = 2, adjusted by H_2SO_4, the scan rate was 5 mV s^{-1}, the RRDE rotation (ω) was 900 rpm and the ring potential (E_r) was +1.0 V. The O_2 reduction waves were subtracted for the background current recorded in N_2-satured electrolyte.

3.3. Study of H_2O_2 generation in the gas diffusion electrode

The results obtained using RRDE system revealed that the addition of Ta_2O_5 on carbon black increase the selectivity for the H_2O_2 electrogeneration (Fig. 5). In order to study the formation of H_2O_2 by this electrocatalyst in more detail, it was quantify the generation of hydrogen peroxide in solution using a gas diffusion electrode. The ORR on GDE occurs at the solid-liquid-gas interface, and allows the generation of H_2O_2 *in situ*. In contrast to planar electrodes, GDEs do not suffer limitations imposed by the concentration of O_2 gas in the bulk of the solution or by the diffusion of molecules to the electrode surface.

The H_2O_2 detection in GDE was performed by sampling the electrolyte and the H_2O_2 electrogeneration at constant potential was quantified spectrophotometrically. Fig. 6 shows the electrogeneration of H_2O_2 as a function of time of electrolysis using GDEs constructed with carbon black either unmodified or modified with Ta_2O_5 nanoparticles and operated with applied potentials in the range −0.5 V to −1.4 V *vs* Ag/AgCl.

For the GDE constructed with carbon black (Fig. 6A), raising the applied potential from −0.5 V to −1.1 V *vs* Ag/AgCl promotes incremental increases in the concentration of H_2O_2 formed. However, although the highest amount of H_2O_2 (19.1 mg L^{-1}) is recorded after 120 min of electrolysis at a potential of −1.1 V, this value must be considered equivalent to that of 19.0 mg L^{-1} obtained after 120 min electrolysis at −1.0 V given that the GDE shows a variation of 6.3 ± 0.8% according to Reis et al. [24]. At more negative potentials, the electrogeneration of H_2O_2 decreases such that at −1.4 V *vs* Ag/AgCl only 11.6 mg L^{-1} of hydrogen peroxide is formed after 120 min of electrolysis.

A similar behavior is observed for the GDE constructed with Ta_2O_5/C (Fig. 6B), in which case increasing the applied potential from −0.5 V *vs* Ag/AgCl lead to increases H_2O_2 production up to a maximum value of 27.9 mg L^{-1} attained after 120 min of electrolysis at −1.0 V. At more negative potentials, the electrogeneration of H_2O_2 decreases with only 9.4 mg L^{-1} of hydrogen peroxide being formed after 120 min of electrolysis at −1.4 V.

Plots showing the final concentration of H_2O_2 achieved at the end of the experiment as a function of the potential applied to the unmodified and modified GDE (Fig. 7) confirm that the electrogeneration of hydrogen peroxide is more efficient with the Ta_2O_5/C electrode over the potential range from −0.5 to −1.4 V *vs* Ag/AgCl. Moreover, the modified GDE generates a maximum concentration

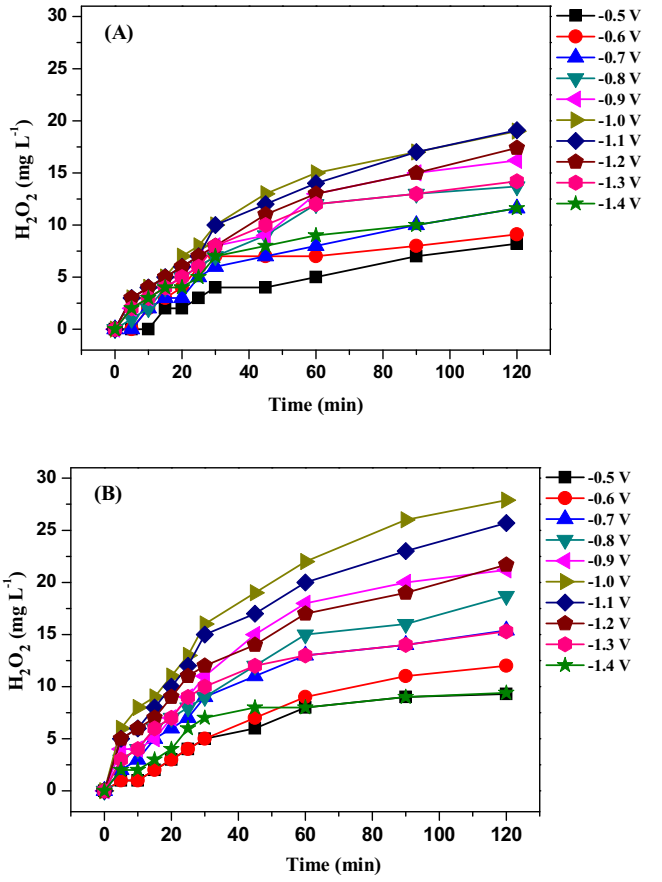

Fig. 6. H_2O_2 electrogeneration in 400 mL of 0.1 mol L^{-1} K_2SO_4 at pH = 2, adjusted by H_2SO_4, and different applied potentials using GDE (3.4 cm^2 exposed area) constructed with (A) unmodified carbon black and (B) carbon black modified with Ta_2O_5 nanoparticles (Ta_2O_5/C).

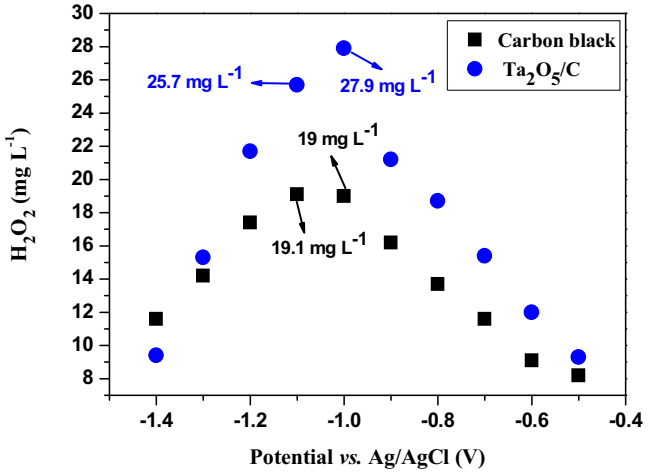

Fig. 7. Final concentrations of H_2O_2 obtained in 400 mL of 0.1 mol L^{-1} K_2SO_4 at pH = 2, adjusted by H_2SO_4, following 120 min of electrolysis using GDE constructed with carbon black and GDE constructed with carbon black modified with Ta_2O_5 nanoparticles.

of H_2O_2 (27.9 mg L^{-1}) at −1.0 V, a value that is 46.1% higher than the maximum level (19.1 mg L^{-1}) produced by the unmodified GDE at −1.1 V.

As may be observed in Fig. 6, the change in H_2O_2 concentration is practically linear during the first minutes of electrolysis indicating that the ORR follows zero-order kinetics. However, modifications in H_2O_2 concentration are related to the cumulative effects of all reactions that occur in parallel with the ORR on the cathode and anode. Thus, the electrosynthesis of H_2O_2 at a GDE is considered to follow global pseudo-zero-order kinetics [9,24,25] and the global rate constant k (mg L^{-1} min^{-1}) can be calculated from the angular coefficients of plots of H_2O_2 concentration (mg L^{-1}) *vs* time (min) considering only the first 30 min of each experiment. The global rate constant for the formation of H_2O_2 (Fig. S5) increases as the applied potential increases from −0.5 V *vs* Ag/AgCl, and attains a maximum of 6.9 mg L^{-1} min^{-1} at −1.1 V with the unmodified GDE and a maximum of 7.6 mg L^{-1} min^{-1} at −1.0 V with the modified GDE. At potentials more negative than −1.1 V, values of k decrease with increasing applied potential for both electrodes. According to Valim et al. [6], decreases in k at applied potentials higher than −1.1 V are associated with increases activity of the ORR by the four-electron transfer mechanism and the consequent decreases in H_2O_2 formation via the two-electron pathway, as verified by the results shown in Fig. 7.

The energy consumption EC (kW h kg^{-1}) for the H_2O_2 electrogeneration [24] plotted as a function of the potential applied to the unmodified and modified GDEs is showed in Supporting information (Fig. S6). Both electrodes exhibit similar behavior up to a potential of −1.1 V *vs* Ag/AgCl, but show greater variation at more negative potentials. EC, which is directly proportional to cell current and potential, increase incrementally up to −1.1 V as the concentration of H_2O_2 generated gradually increase. However, at potentials higher than −1.1 V, the H_2O_2 formation decreases for both electrodes such that the EC values per unit weight of peroxide formed increase markedly, a behavior that has been described previously in the literature [24,25]. In the present study, production of 1 kg of H_2O_2 at the maximum concentration attainable (19.1 mg L^{-1} at −1.1 V) with an unmodified GDE would require 18.8 kWh. However, with the modified GDE, generation of 1 kg of H_2O_2 at maximum concentration attainable (27.9 mg L^{-1} at −1.0 V) would require only 15 kW h.

The high catalytic activity observed with the Ta_2O_5/C electrode can be attributed to the transfer of electrons from Ta_2O_5 to O_2 related to a redox transition in the oxygen reduction region, and to the presence of oxygenated groups on the modified carbon surface (Fig. 2). In this electrocatalyst, the oxygen molecule probably couple to the electrode surface according to the process described by Pauling [8] in which the weak adsorption of O_2 to the metal [26,27] hinders breaking of the O—O bond resulting in the H_2O_2 formation as the final product.

4. Conclusions

Ta_2O_5 nanoparticles on carbon black were prepared by thermal decomposition of a polymeric precursor solution. In addition, carbon black was treated in order to verify the influence of the polymeric precursor method in the carbon catalytic activity for the ORR. The current efficiency for H_2O_2 electrogeneration on Ta_2O_5/C catalyst is 83.2%. The carbon black exhibits an I(H_2O_2)% of 65.3% whereas the treated carbon displays 74.5% yield of H_2O_2 electrogeneration. The high selectivity to H_2O_2 production on Ta_2O_5/C catalyst is attributed to the synergistic effect between the Ta_2O_5 nanoparticles and the oxygen functional groups on the surface of the material. Based on the results obtained in the RRDE system, the H_2O_2 electrogeneration was monitored in detail using a GDE (3.4 cm^2 exposed area) constructed with carbon black either unmodified or modified with Ta_2O_5 nanoparticles. The results confirm the generation behavior observed with RRDE in that the modified GDE produces 27.9 mg L^{-1} of H_2O_2, while the unmodified GDE generates 19.1 mg L^{-1} of H_2O_2. Therefore, the addition of Ta_2O_5 on carbon give rise to an increase in H_2O_2 formation of almost 46.1%. Furthermore, the EC for the H_2O_2 electrogeneration is lower in modified than in unmodified GDE (15 kW h kg^{-1} vs. 18.8 kW h kg^{-1}). Thus, the high performance of the GDE (Ta_2O_5/C) renders it a viable alternative cathode in the electrochemical treatment of contaminated wastewaters.

Acknowledgments

The authors acknowledge the financial support of the Conselho Nacional de Desenvolvimento Científico e Tecnológico (CNPq—grants 163689/2015-6, 160507/2011-1, 143345/2011-7 and 470079/2013-4), the Fundação de Amparo à Pesquisa do Estado de São Paulo (FAPESP—grants 2011/14314-1) and the Coordenação de Aperfeiçoamento de Pessoal de Nível Superior (CAPES).

Appendix A. Supplementary data

Supplementary data associated with this article can be found, in the online version, at http://dx.doi.org/10.1016/j.apcata.2016.03.013.

References

[1] G.V. Buxton, C.L. Greenstock, W.P. Helman, A.B. Ross, W. Tsang, J. Phys. Chem. Ref. Data 17 (1988) 513, http://dx.doi.org/10.1063/1.555805.
[3] W.H. Glaze, J.W. Kang, Ind. Eng. Chem. Res. 28 (1989) 1573–1580, http://dx.doi.org/10.1016/0368-1874(79)87235-4.
[4] E. Brillas, E. Mur, J. Casado, J. Electrochem. Soc. 143 (1996) L49–L53.
[5] M.H.M.T. Assumpção, R.F.B. De Souza, D.C. Rascio, J.C.M. Silva, M.L. Calegaro, I. Gaubeur, et al., Carbon N. Y. 49 (2011) 1842–2851.
[6] R.B. Valim, R.M. Reis, P.S. Castro, A.S. Lima, R.S. Rocha, M. Bertotti, et al., Carbon N. Y. 61 (2013) 236–244, http://dx.doi.org/10.1016/j.carbon.2013.04.100.
[7] E. Yeager, Electrochim. Acta 29 (1984) 1527–1537, http://dx.doi.org/10.1016/0013-4686(84)85006-9.
[8] B.E. Conway, J.O.M. Bockris, E. Yeager, S.U.M. Kham, R.E. White, Comprehensive Treatise of Electrochemistry, vol. 7, Kinetics and Mechanisms of Electrode Processes, New York (1983) ISBN: 978-1-4613-3586-3 (Print) 978-1-4613-3584-9 (Online).
[9] J.C. Forti, R.S. Rocha, M.R.V. Lanza, R. Bertazzoli, J. Electroanal. Chem. 601 (2007) 63–67, http://dx.doi.org/10.1016/j.jelechem.2006.10.023.
[10] F. Xu, T. Song, Y. Xu, Y. Chen, S. Zhu, S. Shen, J. Rare Earths 27 (2009) 128–133, http://dx.doi.org/10.1016/S1002-0721(08)60206-9.
[11] S. Marcotte, D. Villers, N. Guillet, L. Roue, J.P. Dodelet, Electrochim. Acta 50 (2004) 179–188.
[12] T. Oh, J.Y. Kim, Y. Shin, M. Engelhard, K.S. Weil, J. Power Sources 196 (2011) 6099–6103, http://dx.doi.org/10.1016/j.jpowsour.2011.03.058.
[13] J.Y. Kim, T.K. Oh, Y. Shin, J. Bonnett, K.S. Weil, Int. J. Hydrogen Energy 36 (2011) 4557–4564, http://dx.doi.org/10.1016/j.ijhydene.2010.05.016.
[14] T. Ushikubo, K. Wada, Appl. Catal. 67 (1990) 25–38, http://dx.doi.org/10.1016/S0166-9834(00)84429-2.
[15] V.S. Antonin, M.H.M.T. Assumpcao, J.C.M. Silva, L.S. Parreira, M.R.V. Lanza, M.C. Santos, Electrochim. Acta 109 (2013) 245–251, http://dx.doi.org/10.1016/j.electacta.2013.07.078.
[16] M.P. Pechini, N. Adams, Method of preparating lead and alkaline earth titanates and niobates and coating method using the same to form a capacitor, US Patent 3330697 (1967).
[17] W.R.P. Barros, P.C. Franco, J.R. Steter, R.S. Rocha, M.R.V. Lanza, J. Electroanal. Chem. 722–723 (2014) 46–53, http://dx.doi.org/10.1016/j.jelechem.2014.03.027.
[18] A.V. Naumkin, A. Kraut-Vass, S.W. Gaarenstroom, C.J. Powell, NIST X-ray Photoelectron Spectroscopy Database. NIST Standard Database 20, Version 4.1, htttp:/srdata.nist.gov/XPS/.
[19] J.F. Carneiro, M.J. Paulo, M. Siaj, A.C. Tavares, M.R.V. Lanza, J. Catal. 332 (2015) 51–61, http://dx.doi.org/10.1016/j.jcat.2015.08.027.
[20] A. Wang, A. Bonakdarpour, D.P. Wilkinson, E. Gyenge, Electrochim. Acta 66 (2012) 222–229, http://dx.doi.org/10.1016/j.electacta.2012.01.086.
[21] G. Zhang, F. Yang, M. Gao, L. Liu, J. Phys. Chem. C 112 (2008) 8957–8962, http://dx.doi.org/10.1021/jp800757v.
[22] M. Pourbaix, Atlas of Electrochemical Equilibria in Aqueous Solutions, 2nd ed., Texas, USA (1974) ISBN-13: 978-0915567980. ISBN-10: 0915567989.

[23] U.A. Paulus, T.J. Schmidt, H.A. Gasteiger, R.J. Behm, J. Electroanal. Chem. 495 (2001) 134–145, http://dx.doi.org/10.1016/S0022-0728(00)00407-1.
[24] R.M. Reis, A.A.G.F. Beati, R.S. Rocha, M.H.M.T. Assumpção, M.C. Santos, R. Bertazzoli, et al., Ind. Eng. Chem. Res. 51 (2012) 649–654, http://dx.doi.org/10.1021/ie201317u.
[25] W.R.P. Barros, R.M. Reis, R.S. Rocha, M.R.V. Lanza, Electrochim. Acta 104 (2013) 12–18, http://dx.doi.org/10.1016/j.electacta.2013.04.079.
[26] J.R. Kitchin, J.K. Nørskov, M.A. Barteau, J.G. Chen, J. Chem. Phys. 120 (2004) 10240–10246, http://dx.doi.org/10.1063/1.1737365.
[27] J. Zhang, M.B. Vukmirovic, Y. Xu, M. Mavrikakis, R.R. Adzic, Angew. Chem. Int. Ed. 44 (2005) 2132–2135, http://dx.doi.org/10.1002/anie.200462335.